

Synthesis, Spectroscopy and Photochemistry of Nitro-Azobenzene Dyes Bearing Benzophenone Parts

Fang Gao · Jianchao Wang · XiaoJiao Liu · Long Yang ·
Nvdan Hu · Ting Xie · Hongru Li · Shengtao Zhang

Received: 6 June 2008 / Accepted: 3 November 2008 / Published online: 19 November 2008
© Springer Science + Business Media, LLC 2008

Abstract Novel nitro-azobenzene dyes bearing one or two benzophenone branches were proposed and synthesized to improve their photophysical and photochemical properties. The new dyes exhibited double UV/visible bands, and they displayed weak fluorescence emission as excited at 350 nm. Single crystal X-ray diffraction data showed that two phenyl rings of azobenzene was almost coplanar, and the benzophenone part was neither coplanar nor linear connection with azobenzene via ether bridged bond, which have good fit with molecular geometry optimization calculation results. The cyclic voltammetric results of nitro-azobenzene dyes were firstly reported in this paper, which demonstrated that the electrochemical properties of nitro-azobenzene dyes was altered by the substitution of benzophenone part. Thermal stabilities of the new dyes were studied by the analysis of differential scanning calorimetry (DSC) and thermogravimetry (TG) in this paper. Efficient visible-light photoinitiating polymerization of methyl methacrylate (MMA) by the novel nitro-azobenzene dyes was presented and discussed.

Keywords Synthesis · Nitro-azobenzene dye · Benzophenone · Spectroscopy · Electrochemistry · Photochemistry

Introduction

In recent years, the rapidly growing interest in applications of visible-light laser and infrared laser dyes, such as 3-D data

photo-storage and microfabrication, stimulates the studies of long-wavelength and multi-photon photopolymerizations [1–6], since these can be applied widely in optical material and biomedical fields. Intermolecular dye-sensitization was employed to achieve visible-light photopolymerization and multi-photon polymerization [7–9], for instance ultraviolet photoinitiator diaryliodonium salt and dialkylphenacylsulfonium salt could be sensitized by ketone dyes as irradiated by visible light to produce free radicals for the photopolymerization of epoxides and vinyl ethers monomer [10]. It was confirmed that the photochemical efficiency was dependent on the photoinduced electron transfer [11]. Geddes and Lakowicz et al presented strong evidence that photoinduced electron transfer played vital role on the development of new fluorescence sensors [12]. Thus, the use of rapid photoinduced intramolecular electron transfer for the realization of long-wavelength and multi-photon photopolymerizations has become a focus. This requires synthesis of novel dye-linked photoinitiators for visible-light photochemistry [13]. Generally, for such compounds, dye part plays the role of absorption of visible light, and then an efficient photoinduced intramolecular electron transfer occurs between dye part and photoinitiator part resulting in production of free radicals for photopolymerization. Many researchers made contributions to synthesize such compounds, such as coumarin dye-linked borates [14] and cyanine dye-linked bis(trichloromethyl)-1,3,5-triazin [15–17]. On the other hand, development of such molecules with required and ideal properties is always a great challenge for photochemists.

Azobenzene is typical chromophore and its dendrimer has been developed recently [18, 19]. Benzophenone and its derivatives are used as typical Norrish type II ultraviolet photoinitiators for photopolymerization [20–22]. This paper firstly presented the synthesis of nitro-azobenzene derivatives bearing one or two benzophenone branches via ether bond for

F. Gao (✉) · J. Wang · X. Liu · L. Yang · N. Hu · T. Xie · H. Li · S. Zhang
College of Chemistry and Chemical Engineering,
Chongqing University,
Chongqing, China 400044
e-mail: fanggao1971@gmail.com

the improvement of their photophysical and photochemical properties. A comprehensive investigation on the spectroscopy, crystal, electrochemistry, thermal analysis and photochemistry was performed and discussed.

Experimental

Materials

4-Methyl-benzophenone (Fig. 1, compound **1**) was a present from Zhengjiang Zhengdan Chemical Corporation. Other chemicals and reagents were purchased from Chongqing Medical and Chemical Corporation unless otherwise specified. The organic solvents were dried using standard laboratory techniques according to published methods [23]. The starting materials were redistilled or recrystallized before use. Compounds **3** to **6** were synthesized in our laboratory.

Instruments

The UV/visible absorption spectra were recorded with a Cintra spectrophotometer. The emission spectra were checked with Shimadzu RF-531PC spectrofluorophotometer. Rodamin 6G in ethanol ($\Phi=0.94$, 1×10^{-5} mol/L [24]) was used as a reference to determine the fluorescence quantum yields of the compounds herein. The melting point was determined using a Sichuan University 2X-1 melting point apparatus which was uncorrected. Nuclear Magnetic Resonance (NMR) was done at room temperature with a Bruker 500 MHz apparatus with tetramethylsilane (TMS) as internal standard and CDCl_3 as solvent. Element analysis

was detected by CE440 elemental analysis meter from Exeter Analytical Inc..

The fluorescence quantum yields of the compounds in solvents with different polarities are measured based on the following equation [25, 26]:

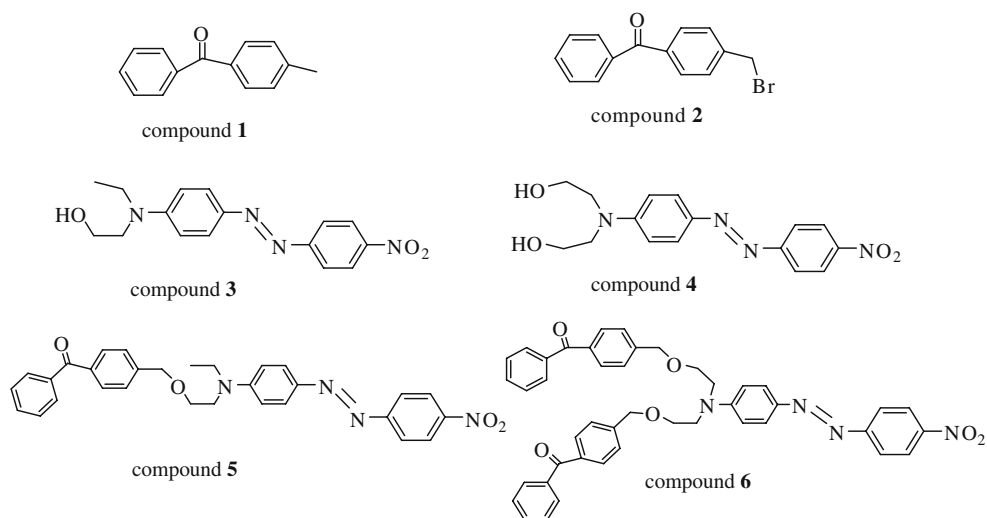
$$\Phi_f = \Phi_f^0 \frac{n_0^2 A^0 \int I_f(\lambda_f) d\lambda_f}{n^2 A \int I_f^0(\lambda_f) d\lambda_f}$$

where n_0 and n are the refractive indices of the solvents, A^0 and A are the absorption at excited wavelength, Φ_f and Φ_f^0 are the quantum yields, and the integrals denote the area of the fluorescence bands for the reference and sample, respectively.

Preparation of single crystals and x-ray crystallography

Single crystal of compound **5** was obtained with slow volatilization of the solvent benzene at 25°C ($C=1 \times 10^{-3}$ mol/L). The crystal structure of the dye was determined by X-ray single crystal diffraction. XRD data were collected on a Bruker-AXS CCD area detector equipped with diffractometer with Mo Ka ($\lambda=0.71073\text{\AA}$) at 298K. A single crystal suitable for determination was mounted inside a glass fiber capillary. The structures of the compounds were solved by direct methods and refined by full-matrix least squares on F^2 . All the hydrogen atoms were added in their calculated positions and all the non-hydrogen atoms were refined with anisotropic temperature factors. SHELXS97 were used to solve the structure and SHELTL were used to refine the structure [27, 28].

Fig. 1 The molecular structures of the compounds involved in this paper



Molecular geometry optimization calculations

Structure optimization was performed with the HyperChem 8.0 package [29] choosing the Indo semiempirical quantum chemical method [30] to keep computations tractable.

Electrochemistry

Electrochemical measurement were carried out using a Shanghai Chenhua working station. Two Pt work electrodes and a Ag/Ag⁺ reference electrode, i.e. three electrodes system, were included in cell. Typically, a 0.05 mol/L solution of tetra-n-butylammonium hexafluorophosphate in CH₂Cl₂ containing of sample was bubbled with argon for 15 min. The scan rate was 0.1 V/s for CV measurements.

Thermal analysis

The differential scanning calorimetry (DSC) and thermogravimetry (TGA) were conducted under N₂ flow in Shimadzu DTG-60H equipment at heating rate 10°C min⁻¹.

Visible-light photochemistry

Nitro-azobenzene dyes (photoinitiators), ethanolamine (as coinitiator) and MMA (monomer) were dissolved in ethyl acetate in dark. Photochemistry was performed in a 10 cm pyrex tube as irradiated by a 1KW tungsten-iodine lamp as

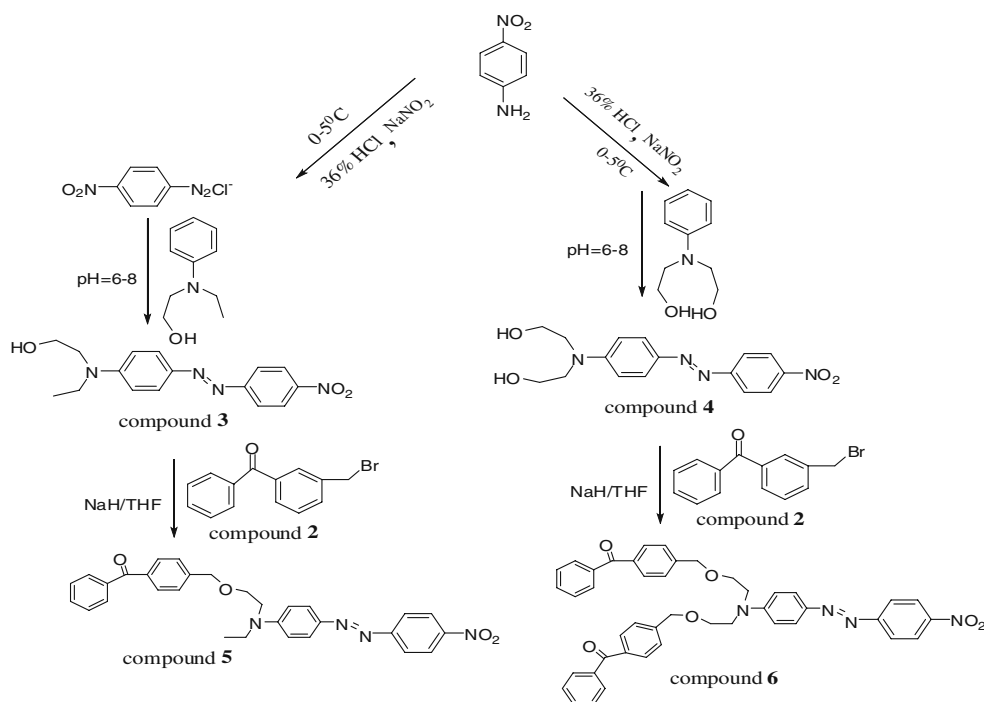
light source at 10 cm distance. The photochemical reaction was kept at room temperature with condenser water and strong fan to eliminate thermo-polymerization. The wavelength below 400 nm was cut off by filter to avoid any UV-light photopolymerization. PMMA is precipitated from cold methanol, and dried by vacuum, and weighted to calculate visible-light photopolymerization yields of MMA.

Synthesis of new nitro-azobenzene dyes

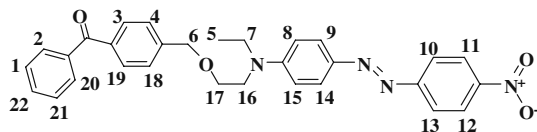
Synthesis route of compounds **5** and **6** was shown in Fig. 2. Precursors Compounds **2**, **3** and **4** were synthesized according to a well-known method with modified procedure respectively [31, 32].

[p-(N-ethyl-N-hydroxyethyl)amino-p'-nitro-azobenzene]-(methylenebenzophone)ether (Compound **5**) was synthesized as followings. 0.4 g (60%, 10 mmol) NaH was washed by dried cyclohexane twice to remove mineral oil. 2.75 g (10 mmol) Compounds **2** and **3** (1.57 g, 5 mmol) were dissolved in NaH/50 ml dried THF, the mixture was stirred at room temperature under argon for 24 h. The solid was got rid of solution by filtration and THF was removed fully by evaporation. The resulting mixture was dissolved in CHCl₃ and washed by water for three times. The organic layer was dried with anhydrous sodium sulfate and then concentrated. The product was purified by column chromatography. Further purification was carried out with twice recrystallization from benzene to yield 0.8 g (1.6 mmol) deep red solid of

Fig. 2 The synthesis route of the compounds **5** and **6**



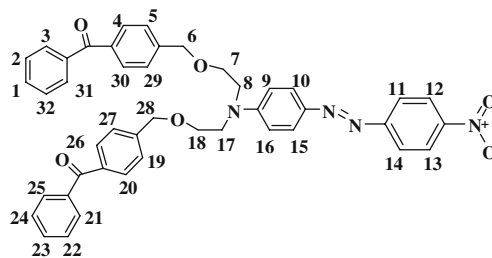
compound **5** (yield 31.5%). $^1\text{H-NMR}$ δ : 1.249–1.277 (t, 1H, **5**), 3.566–3.594 (q, 1H, **7**), 3.710–3.720 (t, 1H, **17**), 3.758–3.779 (t, 1H, **16**), 4.632 (s, 1H, **6**), 6.795–6.812 (d, 2H, **8**, **15**), 7.413–7.456 (d, 2H, **4**, **18**), 7.471–7.487 (d, 2H, **1**, **12**), 7.561–7.576 (d, 1H, **22**), 7.777–7.790 (d, 2H, **3**, **19**), 7.812–7.841 (d, 2H, **2**, **20**), 7.853–7.868 (d, 2H, **10**, **13**), 8.233–8.251 (d, 2H, **11**, **12**), 8.305–8.323 (d, 2H, **9**, **14**). Melting point (94°C), Anal. Calcd for $\text{C}_{30}\text{H}_{28}\text{N}_4\text{O}_4$, C, 70.85, H, 5.55, N, 11.02, O, 12.58. Found: C, 71.12, H, 5.36, N, 11.15.



(number 1-22 stands for the carbon position)

[p-(N,N-dihydroxyethyl)amino-p'-nitro-azobenzene]-(methylenebenzophone) ether (Compound **6**) was prepared as followings. 0.8 g (60%, 20 mmol) NaH was washed by dried cyclohexane twice to remove mineral oil. 5.5 g (20 mmol) Compounds **2** and **4** (1.65 g, 5 mmol) were dissolved in NaH/50 ml dried THF, the mixture was stirred at room temperature under argon for 24 h. The solid was got rid of solution by filtration and THF was removed fully by evaporation. The resulting mixture was dissolved in CHCl_3 and washed by water for three times. The organic layer was dried with anhydrous sodium sulfate and then concentrated. The product was purified by column chromatography. Further purification was carried out with twice recrystallization from benzene to yield 1.22 g (1.7 mmol) deep red solid of compound **6** (yield 34.2%). $^1\text{H-NMR}$ δ : 3.740–3.912 (t, 2H, **7**, **18**), 4.181–4.235 (t, 2H, **8**, **17**), 4.632 (s, 2H, **6**, **28**), 6.814–6.830 (d, 2H, **9**, **16**), 7.378–7.394 (d, 4H, **5**, **19**, **27**, **29**), 7.442–7.473 (d, 4H, **2**, **22**, **24**, **32**), 7.548–7.577 (d, 2H, **1**, **23**), 7.711–7.758 (d, 4H, **4**, **20**,

26, **30**), 7.760–7.768 (d, 4H, **2**, **3**, **25**, **31**), 7.852–7.867 (d, 2H, **11**, **14**), 8.124–8.136 (d, 2H, **12**, **13**), 8.312–8.329 (d, 2H, **10**, **15**). Melting point (52°C), Anal. Calcd for $\text{C}_{44}\text{H}_{38}\text{N}_4\text{O}_6$, C, 73.52, H, 5.33, N, 7.79, O, 13.36. Found: C, 72.93, H, 5.21, N, 7.96.



(number 1-32 stands for the carbon position)

Results and discussion

Spectroscopic properties

UV/Visible spectroscopy

The UV/visible absorption spectra of compounds **5** and **6** reflects their compositions. As shown in Fig. 3, Compounds **5** and **6** exhibited two large absorption bands due to their chemical structures. Obviously, remarkable absorption at short wavelength confirmed the existence of benzophenone part in the molecular structures, and the visible-light absorption arises from nitro-azobenzene chromophore part of the compounds. This demonstrated that benzophenone part was introduced to nitro-azobenzene dye via covalent bond.

Spectral data of compounds **3**, **4**, **5** and **6** in various solvents were presented in Table 1. As shown in Table 1, their long-wavelength absorption displayed bathochromic

Fig. 3 Representative absorption spectra of compound **6** in benzene and CH_3CN ($C=1 \times 10^{-5}$ mol/L)

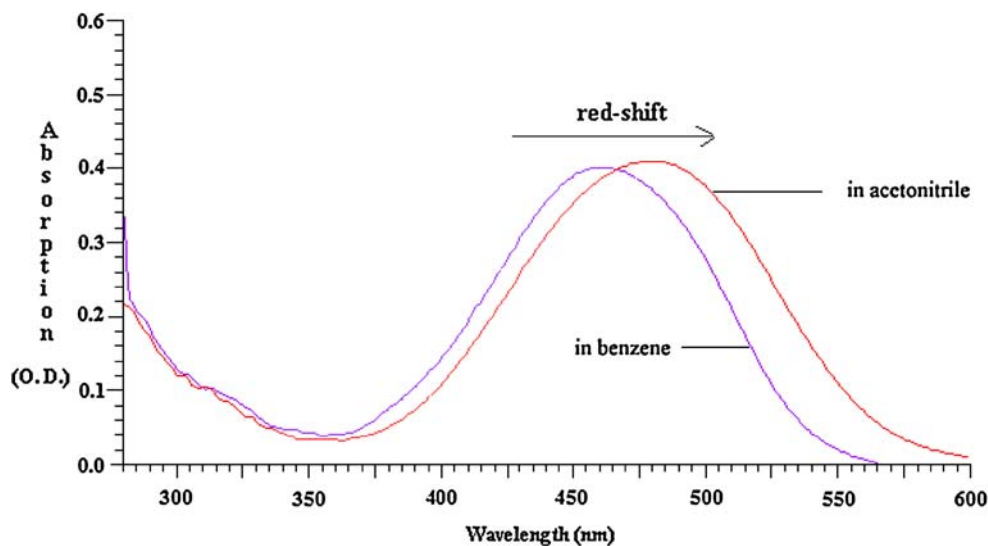


Table 1 Some spectral data of Compounds **3**, **4**, **5**, **6** in various solvents

| Compounds | Solvents | | | | | | | | Dipole moments |
|-----------|------------------|------------|------------------|------------|---------------------------------|------------|--------------------|------------|----------------|
| | Benzene | | Ethyl Acetate | | CH ₂ Cl ₂ | | CH ₃ CN | | |
| | λ_{\max} | ϵ | λ_{\max} | ϵ | λ_{\max} | ϵ | λ_{\max} | ϵ | |
| C3 | 472 | 0.357 | 480 | 0.394 | 482 | 0.357 | 486 | 0.282 | 12.6D |
| C4 | 462 | – | 476 | 0.319 | 470 | 0.270 | 480 | 0.376 | 16.2D |
| C5 | 470 | 0.319 | 474 | 0.362 | 485 | 0.286 | 483 | 0.361 | 11.3D |
| C6 | 460 | 0.428 | 473 | 0.429 | 469 | 0.419 | 479 | 0.426 | 11.6D |

λ_{\max} : nm, ϵ : (1×10^5) L/mol.cm, Dipole moments was calculated for single molecules in vacuum, not in solvents

shift in strong polar solvents. The chemical structure of the compounds **3** to **6** are characterized donor- π -acceptor, which may induce solvent polar effects on their maximal absorption wavelength [33, 34]. Obvious red-shift in strong polar solvents might be due to the intramolecular charge transfer, and the compounds could be characterized with large dipole moment at ground state. We calculated corresponding single molecular dipole moments in vacuum with AM1 method [35], and the results were list in Table 1. Although the calculated dipole moments are not real in solvents, they still reflect basic situation of molecular structures. The single molecules **3**, **4**, **5** and **6** had dipole moments as 12.6D, 16.2D, 11.3D, 11.6D respectively at the ground state in vacuum.

The fluorescence spectroscopy and fluorescence quantum yields

Compounds **3** to **6** showed weak fluorescence emission at 370–575 nm as excited at 350 nm, and they had very similar emission shapes. Representative fluorescence emission spectra of compounds **4** and **6** in THF were shown in Fig. 4. It showed that the introduction of benzophenone part

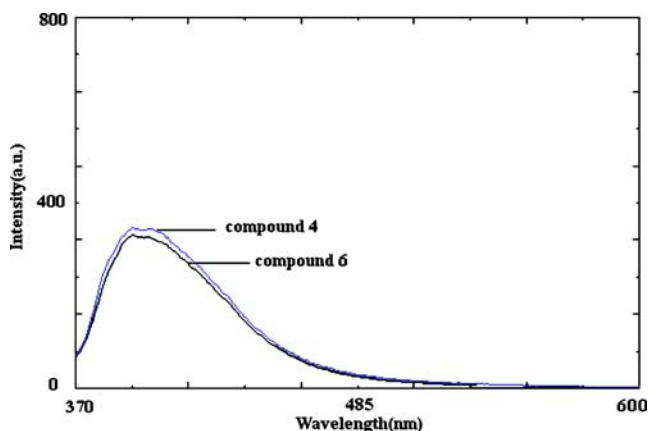


Fig. 4 Representative emission spectra of compounds **4** and **6** in THF. (Ex: 350 nm, Slit Width: Ex: 5 nm, Em: 5 nm)

had no remarkable influence on the fluorescence emission of the nitro-azobenzene. This indicated that the luminescence properties of the compounds were mainly dominated by nitro-azobenzene part. Furthermore, the fluorescence quantum yields of compounds **3** to **6** have been determined in various solvents. The data were presented in Table 2. It showed that four compounds displayed small fluorescence quantum yields in different polar solvents. On the other hand, we noticed that the fluorescence quantum yields of the compounds **5** or **6** were slightly smaller than those of compounds **3** or **4**, which was probably due to the photoinduced intramolecular transfer between two chromophores.

Single crystal x-ray diffraction analysis and molecular structure optimization

Four phenyl rings are included in compound **5**. The crystal data (see “[Supplementary Information Available](#)”) suggested that compound **5** crystallized in the monoclinic system, $P2_1/c$ space group (see Fig. 5).

In the compound **5**, benzene rings C17–C22 and C23–C28 are almost coplanar (dihedral angle: 4°), indicating that they are conjugate (Fig. 5). However, the rings C4–C9 and C11–C16 are deviated from the conjugate plane and the deviated angles are 65.3° and 16.7° , respectively. The dihedral angles between planes C4–C9 and C11–C16 is 53.6° (Fig. 5). Obviously, the benzene rings C4–C9 and C11–C16 of benzophenone part are not linear with benzene rings C17–C22 and C23–C28. These fit well with the

Table 2 The fluorescence quantum yields of Compounds **3**, **4**, **5** and **6**

| Solvents | C 3 | C 4 | C 5 | C 6 |
|---------------------------------|----------------------|----------------------|----------------------|----------------------|
| Benzene | 3.6×10^{-2} | 5.8×10^{-3} | 2.2×10^{-2} | 3.5×10^{-3} |
| THF | 1.6×10^{-2} | 1.9×10^{-2} | 1.4×10^{-2} | 7.3×10^{-3} |
| Ethyl Acetate | 1.1×10^{-2} | 1.5×10^{-3} | 1.2×10^{-2} | 7.2×10^{-3} |
| CH ₂ Cl ₂ | 1.0×10^{-2} | 3.0×10^{-2} | 2.2×10^{-2} | 2.1×10^{-2} |
| Acetonitrile | 1.6×10^{-3} | 4.7×10^{-4} | 1.9×10^{-3} | 1.8×10^{-4} |

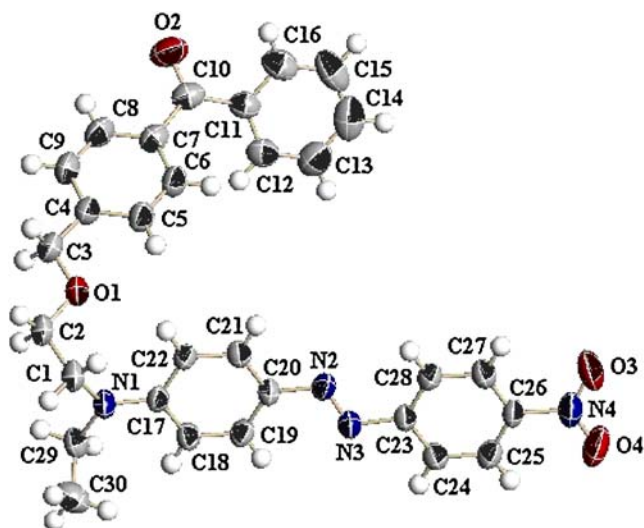


Fig. 5 ORTEP drawing of the compound **5** with thermal ellipsoids at 50% probability

geometry optimization results with Indo semiempirical quantum chemical method by Hyperchem Software. Furthermore, our calculation showed that the benzophenone parts were neither coplanar nor linear connection with azobenzene via ether bridged bond in compound **6** as well. (see Fig. 6)

Electrochemical properties

The cyclic voltammetric data of compounds **5** and **6** were acquired in dichloromethane. For comparison, the electrochemical properties of compounds **3** and **4** were also studied in the same conditions. Generally, the reduction peaks of compounds **5** and **6** exhibited remarkable difference with those of compounds **3** and **4**. The

Fig. 6 Molecular structure optimization of compound **5** (a), and compound **6** (b)

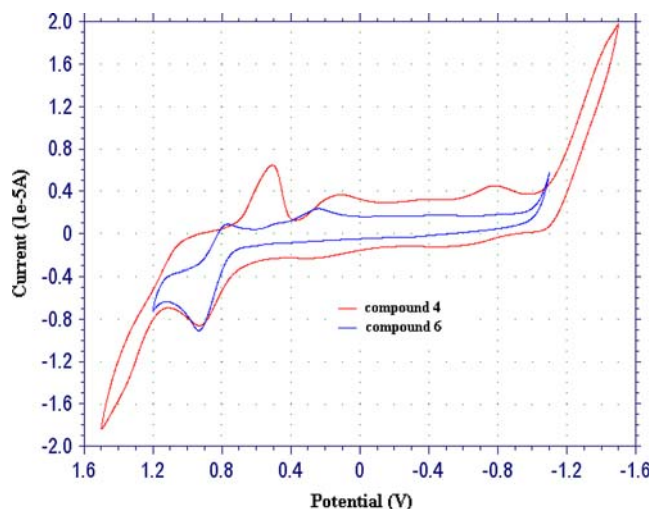
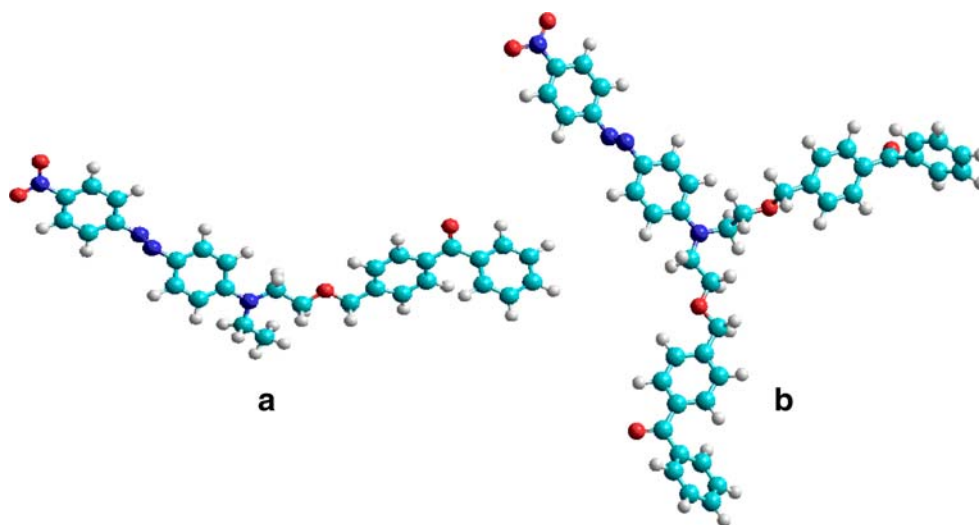


Fig. 7 Cyclic voltammograms of compounds (red line: compound **4**, blue line: compound **6**)

representative voltammograms of compounds **4** and **6** were presented in Fig. 7. From Fig. 7, we found that the cyclic voltammograms of the compounds exhibited irreversible process. Table 3 showed that the electrochemical properties of the nitro-azobenzene were altered by the introduction of benzophenone part. The oxidation peak of compound **5** shifted to a lower potential compared to compound **3**. This suggested that compound **5** was easier to be oxidized than compound **3**. While, in contrast, the oxidation peak of compound **4** was enhanced by the introduction of benzophenone part, while meant that compound **6** was harder to be oxidized than compound **4**. The potential shifts could be due to diminishment or enhancement of HOMO with the introduction of benzophenone.

The ionization potential (IP) and electron affinity (EA) were also estimated based on the corresponding to

Table 3 The electrochemical properties of compounds **3**, **4**, **5**, **6**

| Compounds | E_2^{red} | EA_2 | E_1^{red} | EA_1 | E_1^{ox} | IP_1 |
|-----------|--------------------|--------|--------------------|--------|-------------------|--------|
| C3 | 0.40 | -4.79 | 0.70 | -5.09 | 1.02 | -5.41 |
| C4 | 0.24 | -4.63 | 0.62 | -5.01 | 0.88 | -5.27 |
| C5 | 0.24 | -4.63 | 0.76 | -5.15 | 0.95 | -5.34 |
| C6 | 0.24 | -4.63 | 0.77 | -5.16 | 0.93 | -5.32 |

oxidation and reduction potentials as followings [36, 37]: $IP_n = -eE^{\text{ox}} - 4.39\text{eV}$, $EA_n = -eE^{\text{ox}} - 4.39\text{eV}$. The two parameters denote opposite physical definition. Removal of an electron from the ground state of a molecule is defined as the first ionization potential (IP_1), and this is called the first oxidation process. Further removing another electron from the univalent cation is called the second ionization potential (IP_2), it corresponds to the second oxidation process. Thus similarly, IP_n is the representative of removing multi-electrons. In contrast, the first electron affinity means that the ground state of a molecule obtains an electron, and this corresponds to the first reduction process. The second electron affinity corresponds to the second reduction process. The EA_n has direct association with multi-reduction process. As shown in Table 3, we could postulate that photoinduced intramolecular electron transfer might occur from the nitro-azobenzene part to benzophenone part due to the lower first electron affinity of compounds **5** and **6**. Owing to the short ester spacer bond, the separation from one another of the redox units in compounds **5** and **6** via ester bond may permit larger electronic communication between chromophores.

Thermal analysis

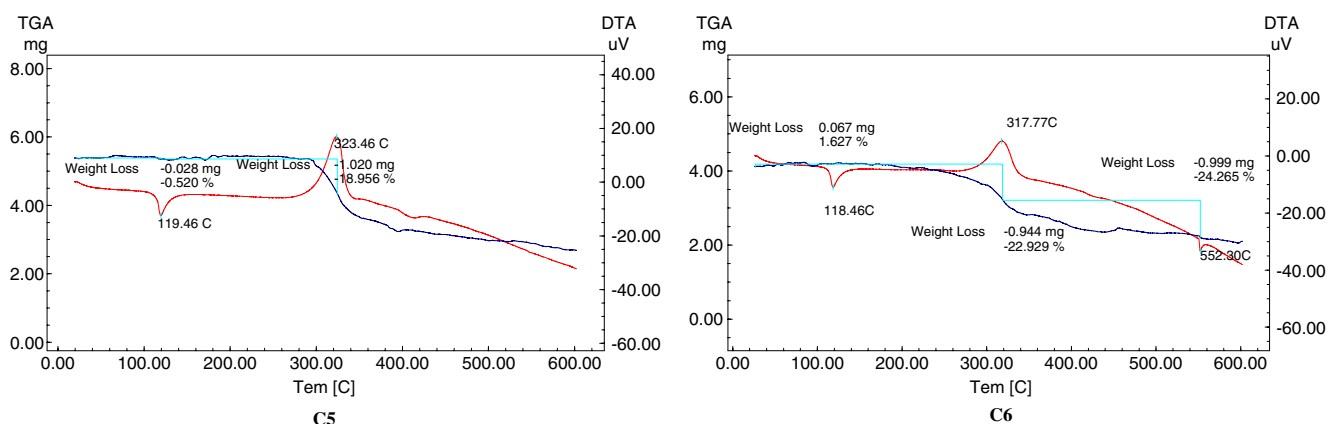
The compounds **5** and **6** exhibited very similar decomposition temperature, which can be observed from their DSC

and TGA curves. **C5** to **C6** display obvious exothermic peak at above 300°C , and weight loss is accompanied with exothermic peak. A Typical DSC and TGA curves of **C5** to **C6** were shown in Fig. 8. The results show that the thermal stability of visible-light photoinitiators **C1** and **C2** is not reduced by the benzophenone moiety. Great thermal stability is big advantage for their further applications.

Visible-Light Photopolymerization

Benzophenone is a typical Norrish II photoinitiator, which has 100% intersystem crossing from excited singlet state to triplet state. It can abstract hydrogen from hydrogen donor, which are used as coinitiator, to produce radicals for photopolymerization during ultraviolet irradiation. In this study, compounds **5** and **6** with benzophenone moiety can efficiently photoinitiate polymerization of acrylate monomer during visible-light irradiation. Our studies showed that when ethanolamine was used as hydrogen donor, even if photoinitiators **5** and **6** were at a very low concentration (lower than 1×10^{-6} mol/L), they could still photoinitiate polymerization of MMA as irradiated by visible light.

For comparisons, we have performed four photosensitive initiating systems for visible-light photochemistry: **P1** (compound **5**, ethanolamine and monomer), **P2** (compound **6**, ethanolamine and monomer), **P3** (compound **1**, compound **3**,

**Fig. 8** The curves of differential scanning calorimetry (DSC) and thermogravimetry (TG) of Compounds **5** and **6**

ethanolamine and monomer), **P4** (compound **1**, compound **4**, ethanolamine and monomer). The plot of MMA photopolymeric ratio of **P2** to **P1** with irradiation time was shown in Fig. 9. It clearly showed that during an hour irradiation, visible-light photoinitiating efficiency of **P2** was larger approximately 1 time than that of **P1**, which demonstrated that the two benzophenone branches induced a more efficient visible-light photopolymerization than one benzophenone branch. The results suggested that “branch effect” played a significant role on the enhancement of visible-light photopolymerization. On the other hand, with the increasing visible-light irradiation time (2 h to 4 h), radical coupling rate might increase due to more free radicals, and this could lead to gradually decrease the ratio of visible-light photoinitiating efficiency of **P2** to **P1**.

We also investigated that compound **1** was sensitized by compounds **3** and **4** for visible-light polymerization. The results suggested that **P3** and **P4** systems could photoinitiate the polymerization of monomer as they were irradiated by visible light, but the photopolymerization yields were low. The plot of MMA photopolymeric ratio of **P1** to **P3** and **P2** to **P4** with the concentration of the photoinitiators was shown in Fig. 10. It clearly showed that during 2 h visible light irradiation, the photopolymerization of MMA ratio of **P2** to **P4** kept around 1.58, and **P3** to **P1** was around 1.41. This indicated that free radicals produced from intramolecular photochemical reaction were much more than those intermolecular photochemical reaction.

It is well known that the efficiency of intramolecular energy or electron transfer is quite high and extends through several covalent linkages when two chromophores are together. The energy transfer occurs only if there is enough overlap of the emission spectroscopy of donor and the absorption spectroscopy of acceptor. In present study, efficient intramolecular energy transfer between chromophore part and benzophenone moiety is highly unlikely due to none overlap of emission of chromophore part and absorption of benzophenone moiety. We assumed that the photoinduced intramolecular and intermolecular electron transfer might occur between nitro-azobenzene chromophore and benzophenone to produce free radicals for photopolymerization as the compound was irradiated by visible-light.

The values of free energy change ΔG for the electron transfer reaction were estimated according to the Rehm-Weller equation [39] and listed in Table 4, wherein nitro-azobenzene as electron donor, benzophenone as acceptor. Negative ΔG indicated that photoinduced electron transfer between nitro-azobenzene and benzophenone had large thermodynamic driving force. As discussed, Table 2 showed that the fluorescence of nitro-azobenzene was slightly quenched by benzophenone part. Thus, we could assume that photoinduced electron transfer occurred tiny partially through the excited single state of the nitro-azobenzene. On the other hand, the weak fluorescence of the nitro-azobenzene indicated that photoinduced electron transfer might occur mainly through excited triplet state of the

Fig. 9 The ratio of the photoinitiating polymerization yields of MMA (**P2** to **P1**) with irradiation time. Wherein: the concentration of compounds **5** and **6** for different lines: **line 1**: 2.5×10^{-7} mol/L, **line 2**: 2×10^{-6} mol/L, **line 3**: 3×10^{-6} mol/L, **line 4**: 4×10^{-6} mol/L, **line 5**: 5×10^{-6} mol/L, MMA: 4.7 mol/L triethanolamine: 2.65 mol/L

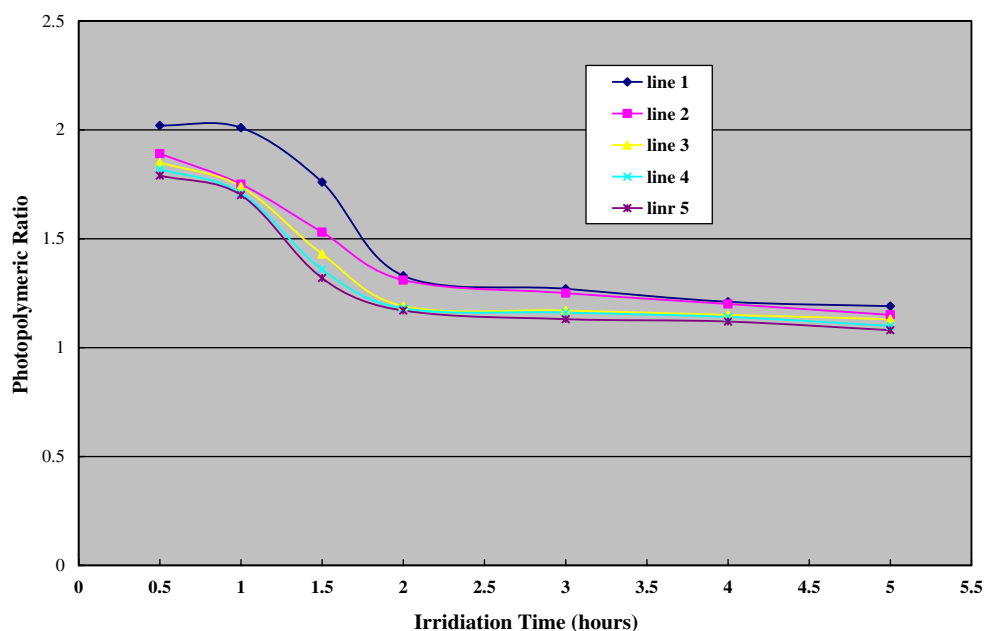
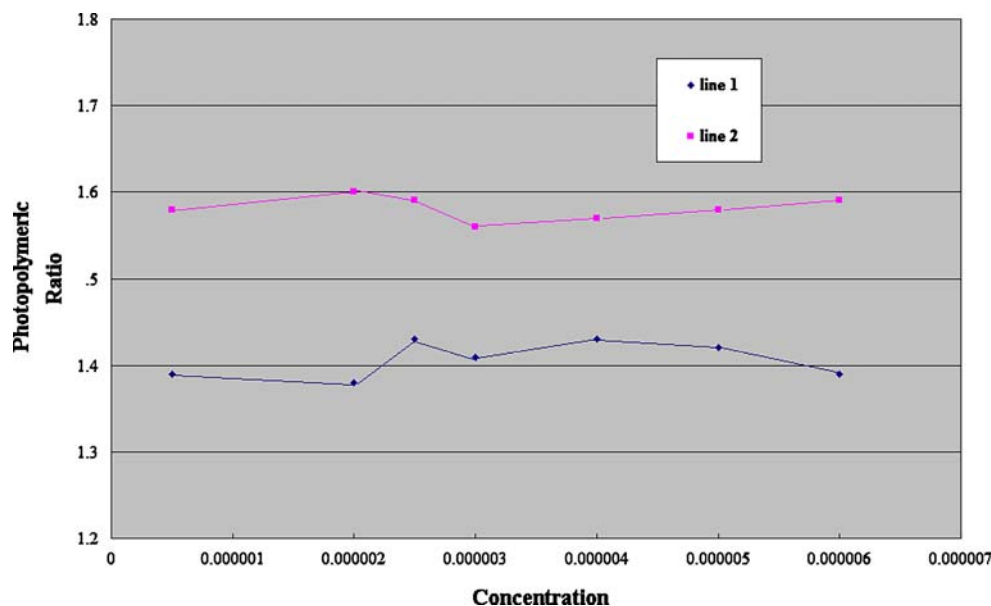


Fig. 10 The ratio of the photo-initiating polymerization yields of MMA (line 1: **P4** to **P2**, line 2: **P3** to **P1**) with different concentration of photoinitiators. Wherein: irradiation time: 2 h, MMA: 4.7 mol/L, triethanolamine: 2.65 mol/L. The concentrations of compounds **1**, **3**, **4**, **5**, **6** are kept same for the survey of each point of the plot



chromophores. This indication is according with the results of literatures [40, 41].

The interaction of benzophenone and triethylamine system under ultraviolet light was well studied, and it was demonstrated that initiating α -aminoketyl free radicals were formed from an exciplex via intermolecular hydrogen transfer [42, 43]. Thus, we proposed photoinitiating process of compound **5** under visible light was shown in Fig. 11. The variations of UV/visible absorption spectra of intramolecular photosensitive initiating systems and intermolecular photosensitive initiating systems with irradiation time were studied and compared. A representative change of UV/visible spectra of **P2** was shown in Fig. 12. It showed that photobleaching of visible-light absorption occurred, and an isobetic point (at 400 nm) and a new absorption band (around 375 nm) were produced with the irradiation time. The intramolecular photosensitive initiating systems displayed more rapid photobleaching than intermolecular photosensitive initiating systems, which in turn explained

Table 4 The estimated values of free energy change ΔG between nitro-azobenzene dye and benzophenone

| Eox(D/D+) | $\Delta E_{0,0(a)}$ | ΔG |
|-------------------|---------------------|-------------|
| C3 1.02 eV | 3.09 | -288 KJ/mol |
| C4 0.88 eV | 2.91 | -280 KJ/mol |

^a $E_{(A/A)}^{\text{red}}$ for benzophenone 0.925 eV [38]; estimation from the fluorescence emission

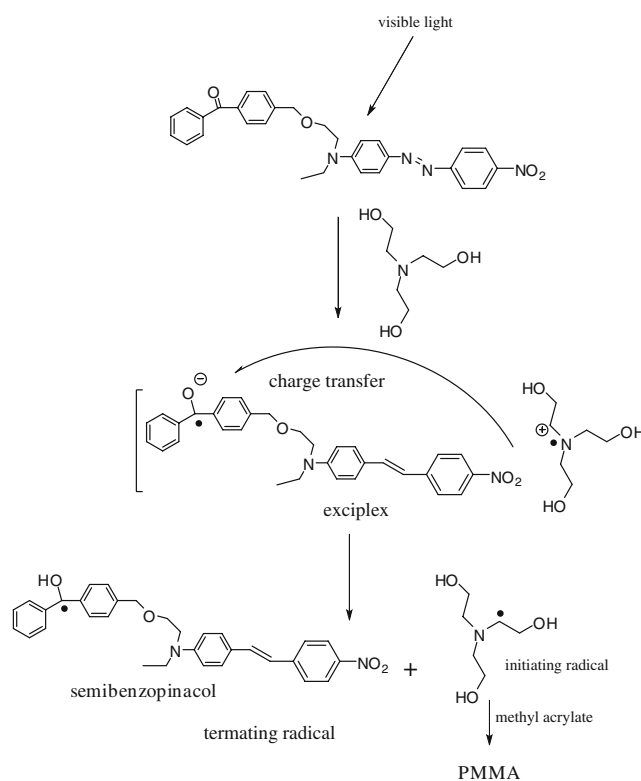
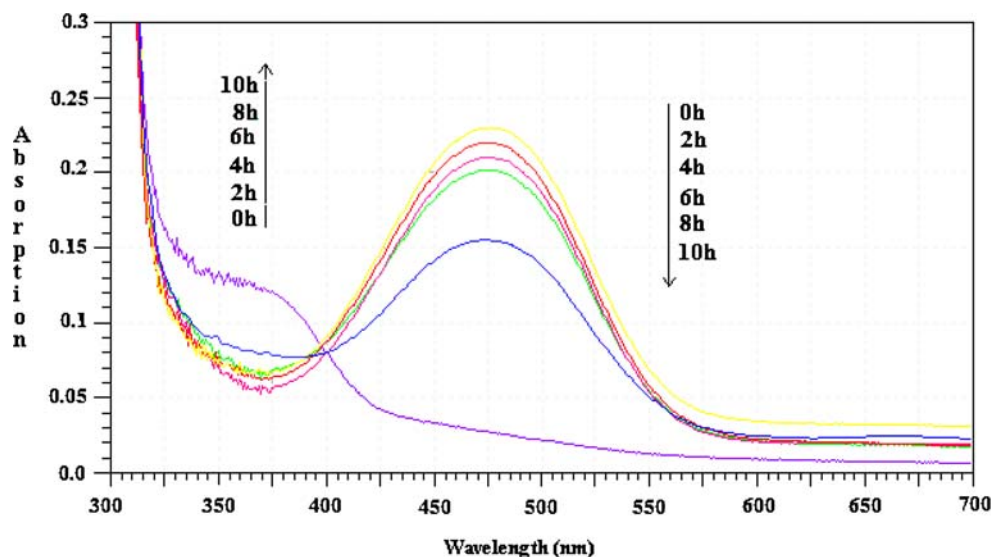


Fig. 11 A proposed photoinitiating polymerization processing of Compound **5**

Fig. 12 The variation of UV/visible absorption spectroscopy of P2 with visible-light irradiation time. Wherein: MMA: 4.7 mol/L, triethanolamine: 2.65 mol/L, the concentrations of compound 6: 53×10^{-6} mol/L, Solvent: ethyl acetate



why the photoinitiating polymerization yields of monomer of **P1** and **P2** were larger than those of **P3** and **P4**.

It is interesting to observe that the effect of coinitiator on the efficiency of photopolymerization was dependent on the amount of branches of triethanolamine. More branches increased the rate of α -aminoketyl free radicals for photopolymerization. Among three ethanolamine derivatives, triethanolamine is the best hydrogen donor. When other experimental conditions were kept the same except for hydrogen donor, we determined the ratio of **P1** and **P2** systems with different coinitiator. The results showed that the photoinitiating polymerization yields of MMA ratio of **P1** system with triethanolamine to the system with diethanolamine was 2.3, and to the system with monoethanolamine was 2.9 times; Similarly, the photoinitiating polymerization yields of MMA ratio of **P2** system with triethanolamine to the system with diethanolamine was 2.2 times, and the system with monoethanolamine was 2.6 times. The results are remarkably consistent.

Conclusions

In summary, this paper describes the synthesis of new nitroazobenzene dyes bearing benzophenone part. Extensive studies have been carried out on the spectral properties, crystal, electrochemical properties, thermal analysis and visible-light photochemistry of the new compounds. Our investigation showed that the introduction of benzophenone part played a significant role on the improvement of the

photoactivity of nitroazobenzene and achievement of rapid intramolecular photoinduced electron transfer. High thermodynamic force promoted the occurrence of this process. The compounds **5** and **6** have great thermal stabilities. The efficient photoinduced intramolecular electron transfer induced efficient visible-light photopolymerization of MMA initiated by the new compounds bearing with benzophenone.

Supplementary information available

CCDC 679944 contains the supplementary crystallographic data for this paper. These data can be obtained free of charge via www.ccdc.cam.ac.uk/conts/retrieving.html or (from the Cambridge Crystallographic Data Centre, 12, Union Road, Cambridge CB2 1EZ, UK; fax: +44 1223 336033).

Acknowledgements The authors thank National Natural Science Foundation of China (NSFC, Nos. 20776165, 20702065 and 20872184) and Natural Science Foundation of CQ CSTC (Nos. CSTC 2007BB4175 and 2007BB4179) for financial supports. The authors thank Key Foundation Project of Chongqing Science and Technology Commission (CSTC 2008BC4020). We also thank “A Foundation for the Author of National Excellent Doctoral Dissertation of PR China (200735)” and “Initiative Funding of Ministry of Personnel of PR China (2006164)” for part of financial support. This paper is part financially sponsored by the Scientific Research Foundation for the Returned Overseas Chinese Scholars, State Education Ministry as well (Nos. 20071108-1, 20071108-5). The authors appreciate Mr. Qingping Feng for his warm support on this project.

References

- Carretero L, Blaya S, Mallavia R, Madrigal RF, Belendez A, Fimia A (1998) Theoretical and experimental study of the bleaching of a dye in a film-polymerization process. *Appl Opt* 37:4496–4499. doi:10.1364/AO.37.004496
- Grotzinger C, Burget D, Jacques P, Fouassier JP (2003) Visible light induced photopolymerization: speeding up the rate of polymerization by using co-initiators in dye/amine photoinitiating systems. *Polymer (Guildf.)* 44(13):3671–3677. doi:10.1016/S0032-3861(03)00286-6
- Mallavia R, Amat-Guerri F, Fimia A, Sastrei R (1994) Synthesis and evaluation as a visible-light polymerization photoinitiator of a new eosin ester with an *o*-Benzoyl- α -oxoimine group. *Macromolecules* 27:2643–2646. doi:10.1021/ma00087a041
- Tasdelen MA, Kumbaraci V, Jockusch S, Turro NJ, Talinli N, Yagci Y (2008) Photoacid generation by stepwise two-photon absorption: photoinitiated cationic polymerization of cyclohexene oxide by using benzodioxinone in the presence of iodonium salt. *Macromolecules* 41(2):295–297. doi:10.1021/ma7023649
- Previtali CM, Bertolotti SG, Neumann MG, Pastre IA, Rufs AM, Encinas MV (1994) Laser flash photolysis study of the photoinitiator system safranin T-aliphatic amines for vinyl polymerization. *Macromolecules* 27:7454–7458. doi:10.1021/ma00103a031
- Zhang S, Li B, Tang L, Wang X, Liu D, Zhou Q (2001) Studies on the near infrared laser induced photopolymerization employing a cyanine dye-borate complex as the photoinitiator. *Polymer (Guildf.)* 42(18):7575–7582. doi:10.1016/S0032-3861(01)00233-6
- Ojah R, Dolui SK (2005) Photopolymerization of methyl methacrylate using dye-sensitized semiconductor based photocatalyst. *J Photochem Photobiol. Chem. (Kyoto)* 172(2):121–125
- Allonas X, Fouassier JP, Kaji M, Miyasaka M, Hidaka T (2001) Two and three component photoinitiating systems based on coumarin derivatives. *Polymer (Guildf.)* 42(18):7627–7634. doi:10.1016/S0032-3861(01)00275-0
- Xing XF, Chen WQ, Gu J, Dong XZ, Takeyasu N, Tanaka T, Duan XM, Kawata S (2007) Design of high efficiency for two-photon polymerization initiator: combination of radical stabilization and large two-photon cross-section achieved by *N*-benzyl 3,6-bis(phenylethynyl)carbazole derivatives. *J. Mater. Chem.* 17:1433–1438. doi:10.1039/b616792f
- Crivello JV, Sangermano M (2001) Visible and long-wavelength photoinitiated cationic polymerization. *J Poly Sci Part A Poly Chem* 39(3):343–356
- Fouassier JP, Allonas X, Burget D (2003) Photopolymerization reactions under visible lights: principle, mechanisms and examples of applications. *Prog Org Coat* 44(13):3671–3677
- Badugu R, Lakowiczand JR, Geddes CD (2005) Fluorescence sensors for monosaccharides based on the 6-methylquinolinium nucleus and boronic acid moiety: potential application to ophthalmic diagnostics. *Talanta* 65(3):762–768. doi:10.1016/j.talanta.2004.08.003
- Kucybala Z, Pyszka I, Packowski J (2000) Development of new dyeing photoinitiators for free radical polymerization based on the 1*H*-pyrazolo[3,4-*b*]quinoxaline skeleton. Part 2. *J Chem Soc Perkin Trans 2*:1559–1567. doi:10.1039/b000583p
- Sarker AM, Kaneko Y, Neckers DC (1998) Photochemistry and photophysics of novel photoinitiators: *N,N,N*-tributyl-*N*-(4-methylene-7-methoxycoumarin) ammonium borates. *J Photochem Photobiol Chem* 117(1):67–74. doi:10.1016/S1010-6030(98)00315-3
- Kawamura K (2004) Novel and efficient dye-linked radical generators for visible light photoinitiating polymerization. *J Photochem Photobiol Chem* 162(2–3):329–338. doi:10.1016/j.nainr.2003.08.013
- Kawamura K Merocyanine-dye-sensitized photoinitiator generating a free-radical via an intramolecular electron-transfer process. *Chem Lett* 32(11):1068–1070. doi:10.1246/cl.2003.1068
- Kawamura K, Kato K (2004) Synthesis and evaluation as a visible-light polymerization photoinitiator of a new dye-linked bis(trichloromethyl)-1,3,5-triazine. *Poly Adv Tech* 15(6):324–328
- Liao L, Stellacci F, McGrath DV (2004) Photoswitchable flexible and shape-persistent dendrimers: comparison of the interplay between a photochromic azobenzene core and dendrimer structure. *J Am Chem Soc* 126(7):2181–2185. doi:10.1021/ja036418p
- Nithyanandhan J, Jayaraman N, Davis R, Das S (2004) Synthesis, fluorescence and photoisomerization studies of azobenzene-functionalized poly(alkyl aryl ether) dendrimers. *Chem Eur J* 10(3):689–698. doi:10.1002/chem.200305297
- Fouassier JP, Allonas X, Lalevee J, Visconti M Radical polymerization activity and mechanistic approach in a new three-component photoinitiating system. *J Poly Sci Part A Poly Chem* 38(24):4531–4541
- Higuchi H, Yamashita T, Horie K, Mitai I (1991) Photo-cross-linking reaction of benzophenone-containing polyimide and its model compounds. *Chem Mater* 3:188–194. doi:10.1021/cm00013a038
- Caldwell RA, Majima T, Pac C (1982) Some structural effects on triplet biradical lifetimes. Norrish II and Paterno-Buchi biradicals. *J Am Chem Soc* 104:629–630. doi:10.1021/ja00366a050
- Perrin DD, Armarego WLF, Perrin DR (1966) Purification of laboratory chemicals. Pergamon, New York
- Fischer M, Georges J (1996) Fluorescence quantum yield of rhodamine 6G in ethanol as a function of concentration using thermal lens spectrometry. *Chem Phys Lett* 260(1–2):115–118. doi:10.1016/0009-2614(96)00838-X
- Maus M, Retigg W, Bonafoux D, Lapouyade R (1999) Photoinduced intramolecular charge transfer in a series of differently twisted donor-acceptor biphenyls as revealed by fluorescence. *J Phys Chem A* 103(18):3388–3401. doi:10.1021/jp9905023
- Lukeman M, Veal D, Wan P, Ranjit V, Munasinghe N, Corrie JET (2004) Photogeneration of 1,5-naphthoquinone methides via excited-state (formal) intramolecular proton transfer (ESIPT) and photodehydration of 1-naphthol derivatives in aqueous solution. *Can J Chem* 82(2):240–253. doi:10.1139/v03-184
- Sheldrick GM (1997) SHELXS 97, Program for crystal structure solution. University of Gottingen, Gottingen
- Sheldrick GM (1997) SHELXL 97, Program for crystal structure refinement. University of Gottingen, Gottingen
- Hyperchem 8.0 Package, Hyperchem Inc., Gainesville, FL
- Pople JA, Beveridge DL, Dobosh PA Molecular orbital theory of the electronic structure of organic compounds. 11. spin densities in paramagnetic species. *J Am Chem Soc* 90(16):4201–4206. doi:10.1021/ja01018a003
- Itoh T, Hall HK (1990) 7-Chloro-7-phenyl-8, 8-dicyanoquinodimethane. A novel initiator for cationic polymerizations. *Macromolecules* 23:4879–4881. doi:10.1021/ma00224a020
- Gubbelmans E, Verbiest T, Picard I, Persoons A, Samyn C (2005) Poly(phenylquinoxalines) for second-order nonlinear optical applications. *Polymer (Guildf.)* 46(6):1784–1795. doi:10.1016/j.polymer.2005.01.001
- Aqad E, Leriche P, Mabon G, Gorgues A, Khodorkovsky V (2001) Novel D- π -A chromophores based on the fulvene accepting moiety. *Org Lett* 3(15):2329–2332. doi:10.1021/ol016143n
- Cumpston BH, Ananthavel SP, Barlow S, Dyer DL, Ehrlich JE, Erskine LL, Heikal AA, Kuebler SM, Lee IYS, McCord-Maughon D, Qin JH, Rockel H, Rumi M, Wu XL, Marder SR, Perry JW

- (1999) Two-photon polymerization initiators for three-dimensional optical data storage and microfabrication. *Nature* 398:51–54. doi:10.1038/17989
35. Dewar MJS, Zebisch EG, Healy EF, Stewart JJP (1985) AM1: a new general purpose quantum mechanical molecular model. *J Am Chem Soc* 107:3902–3909. doi:10.1021/ja00299a024
36. Li Y, Cao Y, Gao J, Wang D, Yu G, Heeger AJ (1999) Electrochemical properties of luminescent polymers and polymer light-emitting electrochemical cells. *Synth. Met.* 99(3):243–248. doi:10.1016/S0379-6779(99)00007-7
37. Tao M, Zhou X, Jing M, Liu D, Xing J (2007) Fluorescence and electrochemical properties of naphthylporphyrins and porphyrin-anthraquinone dyads. *Dyes Pigments* 75(2):408–412. doi:10.1016/j.dyepig.2006.06.022
38. Fawcett WR, Fedurco M (1993) Medium effects in the electroreduction of benzophenone in aprotic Solvents. *J Phys Chem* 97:7075–7080. doi:10.1021/j100129a025
39. Rehm D, Weller A (1970) Kinetics of fluorescence quenching by electron and H₂ atom transfer. 8: 259
40. Jockusch S, Timpe HJ, Schnabel W, Turro NJ (1997) Photoinduced energy and electron transfer between ketone triplets and organic dyes. *J Phys Chem A* 101:440–445. doi:10.1021/jp961744v
41. Yamaji M, Aihara Y, Itoh T, Tobita S, Shizuka H (1994) Thermochemical profiles on hydrogen atom transfer from triplet naphthol and proton-induced electron transfer from triplet methoxynaphthalene to benzophenone via triplet exciplexes studied by laser flash photolysis. *J Phys Chem* 98:7014–7021. doi:10.1021/j100079a021
42. Fouassier JP (1995) Photoinitiation, photopolymerization, and photocuring-fundamentals and applications. Hanser, New York
43. Bhattacharyya K, Das PK (1986) Nanosecond transient processes in the triethylamine quenching of benzophenone triplets in aqueous alkaline media. Substituent effect, ketyl radical deprotonation and secondary photoreduction kinetics. *J Phys Chem* 90:3987–3993. doi:10.1021/j100408a032